Seamless full color holographic printing method based on spatial partitioning of SLM

Article *in* Optics Express · January 2015

DOI: 10.1364/OE.23.000172

Seamless full color holographic printing method based on spatial partitioning of SLM

Youngmin Kim[1], Elena Stoykova[1, 2], Hoonjong Kang[1], Sunghee Hong[1], Joosup Park[1], Jiyong Park[1], and Jisoo Hong[1]

[1]*Realistic Media Platform Research Center, Korea Electronics Technology Institute, 8Floor, #1599, Sangam-dong, Mapo-gu, Seoul 121-835, Korea*
[2]*Institute of Optical Materials and Technologies, Acad.G.Bonchev Str., Bl.109, 1113 Sofia, Bulgaria*

[*]*hoonjongkang@keti.re.kr*

Abstract: The holographic wavefront printer decodes the wavefront coming from a three-dimensional object from a computer generated hologram displayed on a spatial light modulator. By recording this wavefront as an analog volume hologram this printing method is highly suitable for realistic color 3D imaging. We propose in the paper spatial partitioning of the spatial light modulator to perform mosaic delivery of exposures at primary colors for seamless reconstruction of a white light viewable color hologram. The method is verified for a 3×3 color partitioning scheme by a wavefront printer with demagnification of the light beam diffracted from the modulator.

OCIS codes: (090.1705) Color holography; (090.1760) Computer holography; (230.6120) Spatial light modulators.

References and links

1. L. Onural, F. Yaras, and H. Kang, "Digital holographic three-dimensional video displays," Proc. IEEE **99** (4), 576-589 (2011).
2. H. Kang, E. Stoykova, J. Park, S. Hong, and Y. Kim, "Holographic printing of white-light viewable holograms and stereograms", in *Holography - Basic Principles and Contemporary Applications*, E. Mihaylova ed. (InTech 2013), pp. 171-201.
3. J. Hahn, H. Kim, Y. Lim, G. Park, and B. Lee, B**,** "Wide viewing angle dynamic holographic stereogram with a curved array of spatial light modulators," Opt. Express **16** (16), 12372-12386 (2008).
4. F. Yaras, H. Kang, and L. Onural, "Circular holographic video display system," Opt. Express **19** (10)**,** 9147-9156 (2011).
5. T. Kozacki, G. Finke, P. Garbat, W. Zaperty, and M. Kujawinska, "Wide angle holographic display system with spatiotemporal multiplexing," Opt. Express **20** (25), 27473-27481 (2012).
6. M. Yamaguchi, N. Ohyama, T. Honda, "Holographic three-dimensional printer: new method," Appl. Opt. **31** (2), 217-222 (1992).
7. D. Brotherton-Ratcliffe, S. Zacharovas, R. Bakanas, J. Pileckas, A. Nikolskij, J. Kuchin, "Digital holographic printing using pulsed RGB lasers," Opt. Eng. **50** (9), 091307 (2011).
8. H. Yoshikawa, M. Tachinami, "Development of direct fringe printer for computer-generated holograms," in *Practical Holography XVIII: Materials and Applications*, T. H. Jeong and H. I. Bjelkhagen, eds., Proc. SPIE **5742**, 02777-786X (2005).
9. T. Yamaguchi, O. Miyamoto, H. Yoshikawa, "Volume hologram printer to record the wavefront of three-dimensional objects," Opt. Eng. **51** (7), 075802 (2012).
10. H. Kang, E. Stoykova, "Wave-field recording onto a holographic emulsion," presented at Second Korea-Japan Workshop on Digital Holography and Information Photonics, Tokushima, Japan, 19–21 Nov. 2012, http://dhip.i-photonics.jp/.
11. H. Kang, S. Hong, Y. Kim, E. Stoykova, K.-M. Jung, K.-H. Seo, KR Patent 1014231630000 (2014).
12. H. Kang, E. Stoykova, H. Yoshikawa, S. Hong, Y. Kim, "Comparison of system properties for wavefront holographic printers" in *Fringe 2013*, W. Osten, ed. (Springer-Verlag, Berlin-Heidelberg, 2014), pp. 855-858.
13. W. Nishii, K. Matsuashima, "A wavefront printer using phase-only spatial light modulator for producing computer-generated volume holograms" in *Practical Holography XXVIII: Materials and Applications*, H. I. Bjelkhagen and V. M. Bove, eds., Proc. SPIE **9006**, 90061F (2014).

14. K. Hong, J. Yeom, C. Jang, J. Hong, and B. Lee, "Full-color lens-array holographic optical element for three-dimensional optical see-through augmented reality," Opt. Lett. **39** (1), 127-130 (2014).
15. K. Hong, S.-g. Park, J. Yeom, J. Kim, N. Chen, K. Pyun, C. Choi, S. Kim, J. An, H.-S. Lee, U-i. Chung, and B. Lee, "Resolution enhancement of holographic printer using a hogel overlapping method," Opt. Express **21**(12), 14047-14055 (2013).
16. M. Yamaguchi, T. Honda, N. Ohyama, J. Ishikawa, "Multidot recording of rainbow and multicolor holographic stereograms", Opt. Commun. **110** (5-6**),** 523-528 (1994).
17. S. Maruyama, Y. Ono, M. Yamaguchi, "High-density recording of full color full parallax holographic stereogram" in *Practical Holography XXII: Materials and Applications*, H. I. Bjelkhagen and R. K. Kostuk, eds., Proc. SPIE **6912**, 69120N (2008).
18. F. Yang, Y. Murakami, M. Yamaguchi, "Digital color management in full-color holographic three-dimensional printer," Appl. Opt. **51**(19), 4343-4352 (2012).
19. H. Bjelkhagen, E. Mirlis, "Color holography to produce highly realistic three-dimensional images", Appl. Opt. **47** (4), A123-A133 (2008).
20. H. Kang, T. Yamaguchi, H. Yoshikawa, S. C. Kim, E. S. Kim, "Acceleration method of computing a compensated phase-added stereogram on a graphic processing unit", Appl. Opt. **47** (31), 5784–5789 (2008).
21. H. Kang, T. Yamaguchi, and H. Yoshikawa, "Accurate phase-added stereogram to improve the coherent stereogram," Appl. Opt. **47** (19), D44-D54 (2008).
22. H. Kang, E. Stoykova, "Partitioning based fast digital hologram generation method," presented at Third Korea-Japan Workshop on Digital Holography and Information Photonics, Daejeon, Korea 18-20 Nov. 2013, http://cvs.khu.ac.kr/~dhip2013/ .
23. Y. Gentet, P. Gentet, "Ultimate emulsion and its applications: a laboratory-made silver halide emulsion of optimized quality for monochromatic pulsed and full-color holography" in *Holography 2000*, Tung H. Jeong and Werner K. Sobotka, eds., Proc. SPIE **4149**, 56-62 (2000).

1. Introduction

Holography enables capture and reconstruction of the optical field scattered from three-dimensional (3D) objects. A hologram encodes both amplitude and phase of the field under coherent illumination, whereas a photograph records only the amplitude by incoherent light. The 3D visualization feature of holography has aroused expansion of research efforts dedicated to holographic imaging techniques as a holographic display [1] or a holographic printer [2]. The holographic display, which normally uses a diffractive spatial light modulator (SLM) as a display device, has attracted a lot of attention in the 3D display area. However, a wide-viewing angle and fully color expressible holographic display is still way off due to the limited bandwidth of the SLMs [3-5]. In contrast, the holographic printing technique is much closer to immediate plausible applications. The holographic stereogram printers [6], based on inscription of incoherently acquired directional-view images of 3D objects into holographic emulsion as a volume reflection hologram, have already found a market niche [7]. The shortcoming of this holographic printing method is the longitudinally distorted 3D space representation caused by the pinhole camera geometry. Recently, holographic fringe and wavefront printers have been reported which make possible printing from a computer generated hologram (CGH) and provide undistorted reconstruction [2, 8-13]. The fringe printer transfers the input CGH into a holographic emulsion forming a thin hologram; that's why this printing method lacks color selectivity. The holographic wavefront printer decodes the 3D object wavefront from the CGH and records it as an analog volume hologram. Thus this printing method is highly suitable for realistic color 3D imaging [2]. A common feature of all holographic printers is division of the printed hologram into a 2D array of elemental holograms. Information to be recorded in an elemental hologram is displayed on a SLM. Recording of the whole hologram is done by successive exposure of all elemental holograms using a motorized X-Y translation stage. Up to now, most of the printers work with a silver-halide or polymer light-sensitive emulsion [2, 6-13].

Research on holographic printing technology focuses on achieving high-quality imaging and improving printer's performance. The issues like diffraction efficiency, color reproduction, lateral resolution in images, writing time are among the high-priority topics [14-18]. Quality of full color reproduction as a crucial component of imaging quality depends on the way the holographic recording is performed [16-19]. Exposure at three laser wavelengths in

the red (R), green (G), and blue (B) spectral regions in a full color holographic printer can be accomplished in two ways: delivery of multiple exposures from the R, G and B laser sources to each elemental hologram or mosaic delivery of primary colors by spatial division of exposures from the R, G and B lasers. The main drawback of the multiple exposure method is the crosstalk between the color channels that renders difficult satisfactory full color holographic imaging [18]. Spatially divided RGB mosaic recording shows robustness to the crosstalk at the expense of gaps in information displayed by each color channel that may hamper smooth color reproduction. Decrease of the gaps means decrease of the elemental hologram size which, at least theoretically, could be as large as the SLM active area for the fringe or wavefront printers. In practice, however, this size should be kept rather small to compensate for inevitable imperfections during the recording of the hologram that may cause reconstruction with artifacts like stripes superimposed on the reconstructed image [8, 9, 13]. Mosaic delivery also imposes limitations on the elemental hologram size that may entail usage of high-end optical components. Apart from being expensive, such solution increases the writing time.

In this paper we propose how to improve color reproduction of the wavefront printer at mosaic delivery without decreasing the elemental hologram size. Seamless color reconstruction is achieved by spatial partitioning of the SLM in order to record a color mosaic of sub-elemental holograms within a single elemental hologram. The proposed method is verified experimentally with the developed by us color wavefront printer at partitioning the elemental hologram as a 3 × 3 array of sub-elemental holograms. Each sub-elemental hologram corresponds to a single color. The paper is organized as follows: in Sec. 2 we discuss the wavefront printing method from the point of view of mosaic delivery of RGB exposures; in Sec. 3 we introduce the spatial partitioning scheme of the SLM; in the last Sec. 4 the principle of the proposed method is verified experimentally, and its feasibility is confirmed.

2. Wavefront printing method.

The holographic wavefront printing is based on extraction of the light beam carrying information about the 3D object from a CGH. This CGH is a 2D array of real numbers that encode the interference at the hologram plane (ξ,η) of the object wave with a complex amplitude, $\boldsymbol{O}(\xi,\eta)=a_O(\xi,\eta)\exp[i\varphi_O(\xi,\eta)]$ and the mutually coherent reference wave, $\boldsymbol{R}(\xi,\eta)=a_R(\xi,\eta)\exp[i\varphi_R(\xi,\eta)]$ where $a_{O,R}$ and $\varphi_{O,R}$ are the amplitudes and phases of these waves. In general, four terms are superimposed at the plane of the hologram

$$H(\xi,\eta)=\left|\boldsymbol{R}(\xi,\eta)+\boldsymbol{O}(\xi,\eta)\right|^2=\boldsymbol{R}\boldsymbol{R}^*+\boldsymbol{O}\boldsymbol{O}^*+\boldsymbol{O}\boldsymbol{R}^*+\boldsymbol{O}^*\boldsymbol{R} \tag{1}$$

where the asterisk denotes a complex conjugate operator. The first and the second terms are the intensities of the reference and object waves that form the zero-order term. The last two terms represent +1 and -1 diffraction orders which encode the relevant information and form the so called twin images. Multiplication of $H(\xi,\eta)$ in (1) with the replica of $\boldsymbol{R}$ or its conjugate reconstructs the object field $\boldsymbol{O}\boldsymbol{R}^*\boldsymbol{R}=\boldsymbol{O}$ or $\boldsymbol{O}^*\boldsymbol{R}^*\boldsymbol{R}=\boldsymbol{O}^*$, and brings into focus the virtual or the real image. A plane wave, $\boldsymbol{R}$, in generation of the CGH and reconstruction produces non-distorted virtual and real images. The twin images are separated for the off-axis geometry in which the light beams $\boldsymbol{R}$ and $\boldsymbol{O}$ subtend a certain angle. The CGH is displayed by a SLM and modulates the light wave it diffracts. In general, the SLM is illuminated by a plane wave falling normally to its surface. In case of a phase-only SLM only the phase of one of the diffraction orders is fed to the SLM. Extraction of the object wave field is made by spatial filtering. For the purpose, the light diffracted from the SLM is collected by a lens in whose rear focal plane the light distribution correspond to the spectrum of the hologram in the spatial frequency domain (u,v)

$$I(u,v)=F\left\{\boldsymbol{RR}^{*}+\boldsymbol{OO}^{*}+\boldsymbol{OR}^{*}+\boldsymbol{O}^{*}\boldsymbol{R}\right\}=I_{R}^{0}+I_{O}^{0}+I_{v}^{1}+I_{r}^{1} \tag{2}$$

Here F is a Fourier transform, $I_{R,O}^{0}$ are the spectra of the reference and object beams intensities while $I_{v,r}^{1}$ give the spectra of the virtual and real image terms. The terms I_{O}^{0} and I_{R}^{0} are located around the zero frequency in the Fourier domain or around the optical axis. Introduction of a spatial carrier frequency in calculation of the CGH by tilting the reference beam with respect to the hologram-to-object observation axis separates spatially $I_{R,O}^{0}$ from I_{v}^{1} and I_{r}^{1}. A filter in the rear focal plane that is shifted with respect to the optical axis cuts off the undesired components such as the -1st order diffracted wave and the non-diffracted wave for an amplitude SLM [2, 9-12] or a phase noise for a phase-only SLM [13]. The filtered light beam interferes with the mutually coherent reference beam within the holographic emulsion to record a volume elemental hologram. Note that there are actually three reference waves in the wavefront printer with an amplitude type SLM: the digital reference wave $\boldsymbol{R}$ inclined to the CGH's plane, the optical plane wave illuminating the SLM and the mutually coherent plane wave which illuminates the exposed area in the holographic plate from the opposite side to form a thick reflection hologram in the photo-sensitive layer of the plate.

The size of the elemental hologram is determined by the way the CGH has been calculated and by the optical system used to form the object beam. The printer in [9] uses an amplitude SLM with resolution of 1920 × 1080 pixels and pixel interval of 7 μm. The filtered 1st diffraction order is reimaged by a $4f$ system onto a converging lens. This lens is required to reconstruct the image of a small part of the object in the vicinity of the holographic plate from the SLM fringe pattern calculated as a lensless Fourier hologram. For calculation of the CGH a spatial window is put in front of the object which is represented as a point cloud of self-illuminated points. The reference point source is positioned at the plane of the object within the spatial window. The CGH is computed following the Rayleigh-Sommerfeld (R-S) diffraction model with

$$\boldsymbol{O}(\xi,\eta)=\sum_{p=1}^{P}A_{p}r_{p}^{-1}\exp\left(jkr_{p}\right) \tag{3},$$

where (x_p, y_p, z_p) are the Cartesian coordinates of the p-th object point, $A_p = a_p \exp(j\phi_p)$ with a_p and ϕ_p being the amplitude and the phase of the light field emanated by this point, and $r_p = \sqrt{(\xi - x_p)^2 + (\eta - y_p)^2 + z_p^2}$ is the distance between this point and the point on the CGH ; $k = 2\pi/\lambda$ is a wave number, λ is the wavelength, and P is the number of points. The size of the elemental hologram in [9] is 2 mm × 1.4 mm.

The wavefront printer built by us also employs amplitude SLM. The input CGH can be calculated with a plane or spherical reference wave. The object is located at a distance from the hologram plane, and all points from the object contribute to the elemental hologram. This sets as a mandatory requirement usage of a high-resolution SLM. As a consequence of that it is beneficial to replace the R-S computation of the CGH by a phase-added stereogram approach in its various modifications [20-22]. We used in this paper the fast phase-added stereogram (FPAS) method with a plane reference wave [22]. To generate the fringe pattern the elemental hologram in the hologram plane (ξ,η) is divided into $M \times N$ square segments of size $Q \times Q$ pixels each. The numerical model of the FPAS in each segment is expressed as

$$H_{mn}(\xi,\eta)=F^{-1}\{I_{mn}(u,v)\}, \tag{4}$$

$$I_{mn}(u,v)=\sum_{p=1}^{P}\frac{a_p}{r_{pmn}}\exp\left[j\left(kr_{pmn}+\phi_p\right)\right]\exp\left\{j2\pi\left[u_{pmn}\left(\xi_{cmn}-x_p\right)+v_{pmn}\left(\eta_{cmn}-y_p\right)\right]\times\right\} \times\delta\left(u-u_{pmn},v-v_{pmn}\right) \tag{5}$$

where $H_{mn}(\xi,\eta)$ is the holographic fringe pattern in the *mn*-th segment, and $I_{mn}(u,v)$ is its spatial frequency distribution in the spatial frequency domain; F denotes a Fourier transform. The distance r_{pmn} is determined with respect to the segment central point (ξ_{cmn},η_{cmn}). This is valid also for the spatial frequencies u_{pmn} and v_{pmn} which are given by $u_{pmn}=\lambda^{-1}(\sin\theta_{\xi pmn}-\sin\theta_{r\xi})$ and $v_{pmn}=\lambda^{-1}(\sin\theta_{\eta pmn}-\sin\theta_{r\eta})$, where $\theta_{\xi pmn}$ and $\theta_{\eta pmn}$ are the incident angles from the *p*-th object point to the central point of the segment, and $\theta_{\xi r}$ and $\theta_{\eta r}$ are the illuminating angles of the plane reference wave $R(\xi,\eta)=\exp\{jk(\xi\sin\theta_{\xi r}+\eta\sin\theta_{\eta r})\}$ with respect to the ξ and η axes. The segment size is determined from the requirement to provide quality of reconstruction close to that observed for a CGH computed by a R-S model. The applied fast Fourier transform in Eq. (4) was computed with zero-padding for a number of pixels larger than $Q\times Q$ to decrease the error due to discretization of the spatial frequencies.

The schematic of the optical head of the printer is shown in Fig. 1. The filtered 1st order wavefront is demagnified by a telecentric system consisting of lenses L_1 and L_2 with focal distances f_1 and f_2, and we have $f_2 < f_1$. The holographic emulsion is placed at the focus of the lens L_2. The telecentric lens demagnification is $M = f_2/f_1$, and the size of the elemental hologram is $S_{EH} = MS_{SLM}$, where S_{SLM} is the size of the CGH displayed on the SLM.

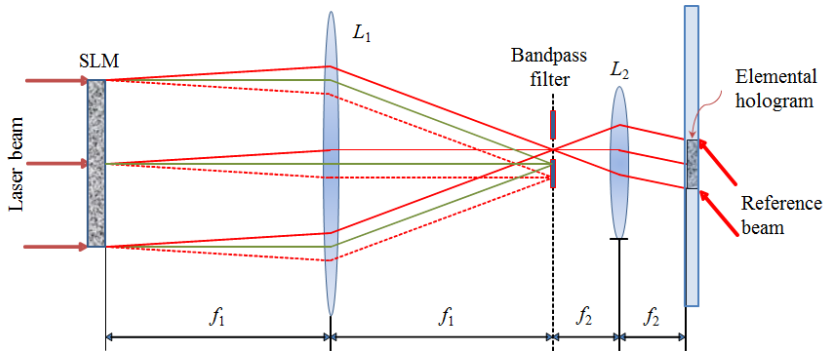

Fig. 1. Holographic wavefront printer with extraction and demagnification of the first diffraction order of the object field encoded in a CGH displayed on amplitude SLM.

3. Wavefront printer with spatial partitioning of the SLM

In contrast to the holographic stereogram printer where the elemental hologram acts as a point emitting in all directions within the viewing angle, the elemental hologram in the wavefront printer is just a part of the hologram that could be bigger or smaller. Actually, the elemental hologram is that hologram part which is recorded at a given position of the X-Y stage. If all object points are used to calculate the CGH fed to the SLM and if the color recording is made by delivery of multiple R, G, B exposures within the same spot, the size of the elemental hologram in the wavefront printer theoretically is restricted by the active area of the SLM. Inevitable imperfections of the recording process, however, as e.g. non-uniform distribution of the light intensity within the laser beam, will cause appearance of a grid superimposed on the reconstructed image if the size of the elemental hologram is too large. The size should be

small also for applying a mosaic exposure method to make a full color hologram as is shown in Fig.2. The figure corresponds to forming the elemental hologram by the optical system in Fig.1. The output hologram is a 2D array of elemental holograms described by their indices. In case of mosaic delivery, the elemental hologram (1, 1) records only the red component of the fringe pattern calculated for it by using Eqs. (4)-(5) at the wavelengths of recording. The elemental hologram (1, 2) takes only the green component of the pattern computed for (1, 2), while (1, 3) – only the blue component of the pattern fed to the SLM to produce (1, 3). Correspondingly, (2, 1) takes only the green component of (2, 1), (2, 2) and (3, 1) – the blue components, (2, 3) – the red component etc. until the color mosaic is formed. Each color component is characterized with a separate set of amplitudes and spatial frequencies $\{a_p, u_p, v_p\}, p = 1..P$ which depend on the wavelength. As the size of the elemental hologram is limited by the used optics, its demagnification ratio M should be very small to make a high quality hologram with smooth perception of colors at reconstruction. Using high-end optical components to achieve greater demagnification with a new demagnification ratio $M' < M$ is expensive solution, which in addition entails $(M/M')^2$ times increase in the writing time.

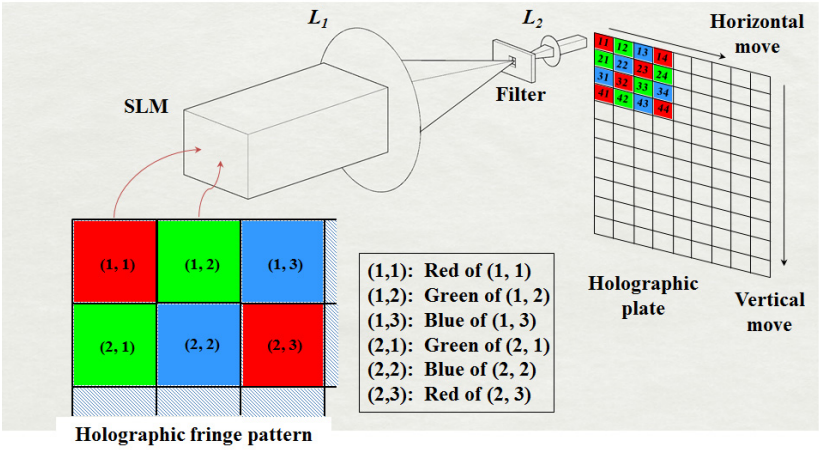

Fig. 2. Schematic of conventional mosaic delivery of exposures at primary colors in a wavefront holographic printer

To find simple and effective solution to demagnification issue, we propose a spatially multiplexed color elemental hologram. The solution is based on the holographic principle itself. The elemental hologram records a CGH which is spatially partitioned into color fragments or sub-elemental holograms of the same size that contain the fringe patterns calculated at the used three wavelengths. Figure 3 shows recording of the elemental hologram with the same optics as in Fig. 2, but now this hologram is formed as a 3 × 3 array of single color fragments. For example, the active area of the SLM for the elemental hologram (1, 1) is partitioned into three fragments corresponding to the red channel of the CGH (1, 1), three fragments - to the green channel and three fragments – to the blue channel. They are arranged as a mosaic, so the fragment corresponding to a given color has borders only with the fragments of the other two colors. The succession of fringe patterns fed to the SLM is depicted in Fig. 4. As is seen, the non-zero values are fed only to the SLM pixels which carry the CGH's parts for the color to be recorded. The laser beam diffracted from the SLM exits the telecentric system after the filtering and demagnification as three separate beams which interfere with the reference beam in the plane of the hologram, as is shown in Fig. 5. Note that the reference beam covers the whole elemental hologram but the interference and hence forming of the fringe pattern occur only where the object beams impinge the holographic plate. Illumination of the remaining

area by the reference beam may lead to some increase of the noise level at reconstruction but it is insubstantial. Thus recording of the elemental hologram at the primary colors is done without inserting spatial masks in front of the reference beams which makes the proposed method easy to apply. Eventually, no part of the elemental hologram remains unexposed both by the object and reference beams. Calculation of the CGH for a given color is made only for the pixels which encode this CGH. The scalable size of the sub-elemental hologram does not depend anymore on the used optics. For example, only a fraction of the SLM pixels may form the elemental hologram.

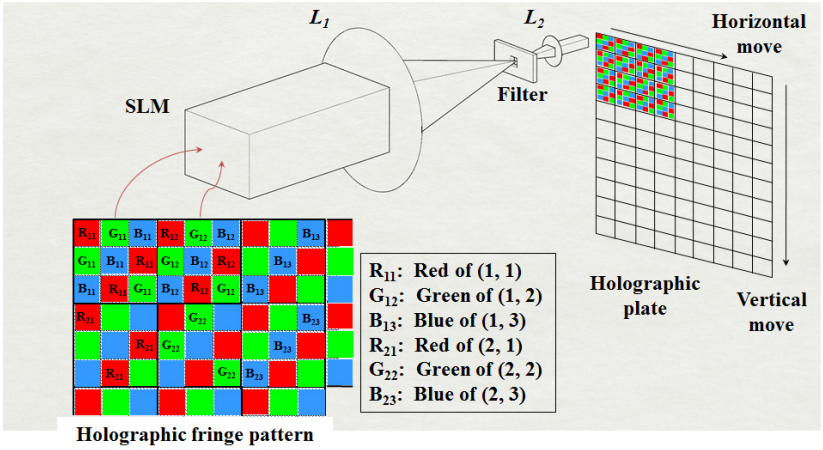

Fig. 3. Schematic of mosaic delivery of exposures at primary colors in a wavefront holographic printer by spatial partitioning of the SLM

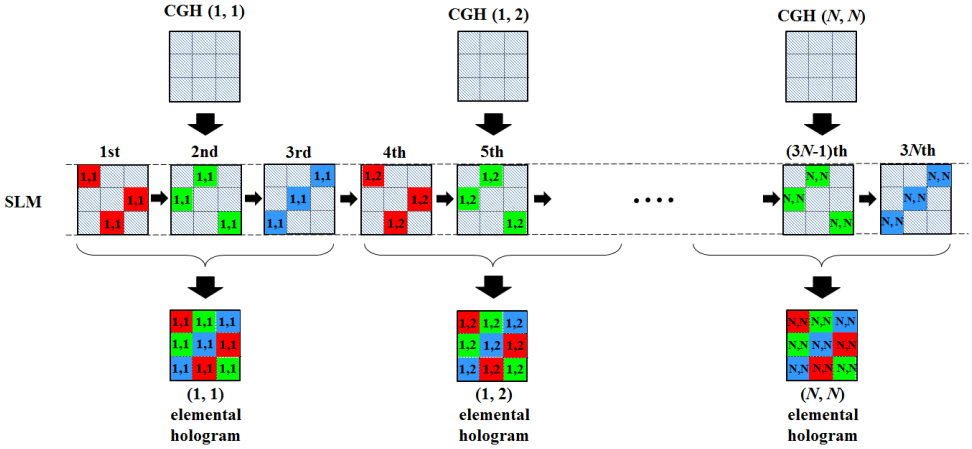

Fig. 4. Succession of grey-scale fringe patterns fed to the SLM and the fringe patterns recorded as elemental holograms.

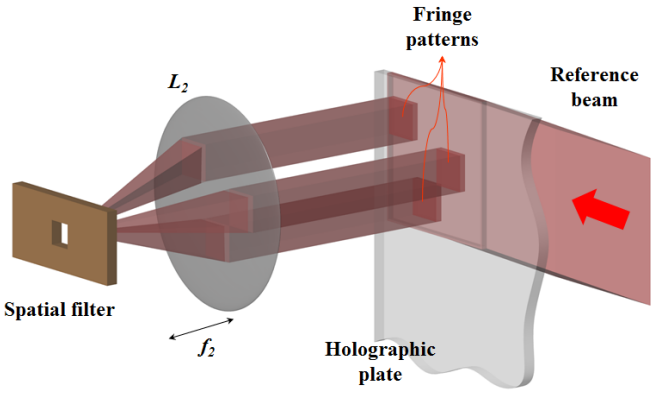

Fig.5. Recording of fringe patterns corresponding to the red channel in the CGH in the elemental volume hologram; the CGH is displayed on a SLM partitioned as a 3 × 3 RGB array.

In addition to simplicity of implementation, another essential advantage of the SLM partitioning scheme for a holographic printer with continuous wave lasers is practically the same writing time as that required for the conventional mosaic recording (Fig. 2). In the latter case, the writing time of a single elemental hologram is a sum of the time interval, t', needed for the shift of the holographic plate to a new position and for the system to settle, and the time interval, t'', needed for loading the CGH on the SLM and for firing the laser. If t' is a portion of a second and t'' for powerful lasers is of the order of ten milliseconds, several times increase in t'' impacts the overall writing time to a much lesser extent than the increase in t'. Increase of t' is observed for the system where the size of the elemental hologram is decreased by optical means.

4. Experimental check

We checked the proposed seamless printing method by using the color wavefront printer whose optical set-up is given in Fig.6. Three continuous wave DPSS lasers emitting at 640 nm, 532 nm and 473 nm were used for color recording. The collimating system sent the beam from each laser onto the first polarizing beam splitter (PBS_1) which formed the object and reference beams for illuminating a single elemental hologram. The laser beam passing through the PBS_1 was the reference beam. The reflected beam was the object beam which illuminated the amplitude type SLM by means of the PBS_2. As a SLM, we used liquid crystal on silicon projector Sony VPL-HW10 SXRD with a number of pixels 1920 × 1080 and a pixel interval 7 μm. The fringe pattern fed to the SLM modulated spatially the object beam which, after filtering and demagnification by the telecentric lens system with a demagnification ratio M = 0.064, impinged the holographic plate from the opposite side to the reference beam. We used extra-fine grain silver-halide emulsion Ultimate08 [23]. The demagnified pixel interval at the plane of the hologram was 0.42 μm. This corresponded to diffraction angle of ± 39.3°. The holographic plate was moved by a X-Y stage at precision of 1 μm along the horizontal and vertical axes at a spatial step, which coincided with the size of the elemental hologram. The size was chosen to be 0.38 mm by 0.38 mm by using only 852 × 852 pixels in the SLM to project CGHs (Fig. 7a). This was done to ensure uniform illumination of the CGH on the SLM without decreasing too much the intensity within the laser beam. The SLM size was $S_{SLM} = 13.44 \times 7.56$ mm^2. The used in the experiment SLM partitioning for projecting the grey-scale patterns for the R, G, B channels of the CGH recorded as an elemental hologram is depicted in Fig.7(b). The sub-elemental holograms size was 0.127 mm × 0.127 mm, and was

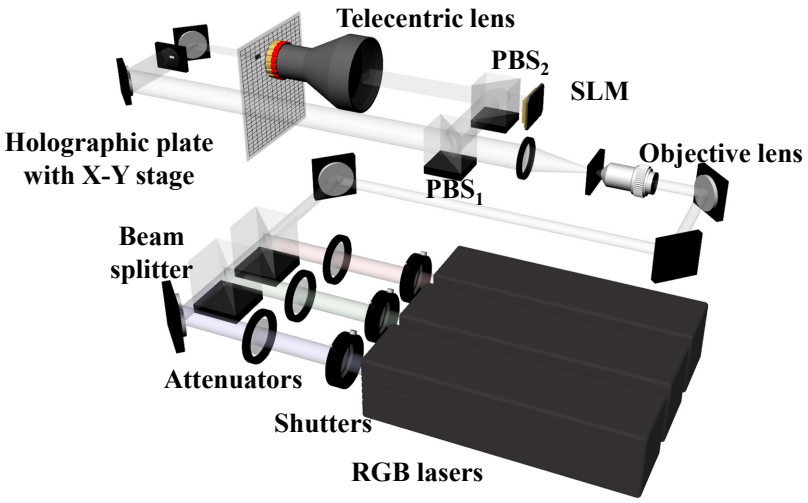

Fig. 6. Optical set-up of a color wavefront printer with telecentric optics; PBS - polarizing beam splitter.

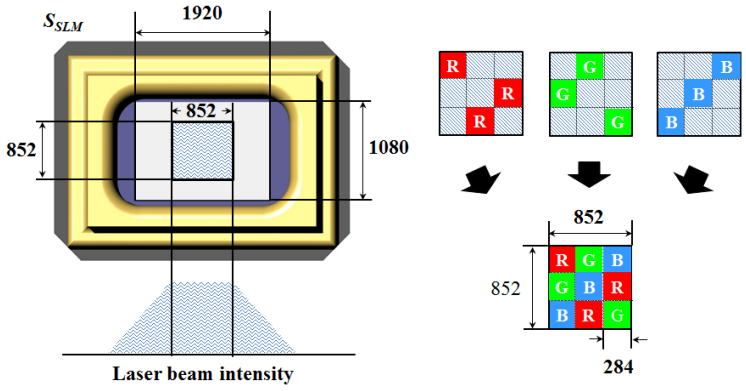

(a) (b)

Fig. 7. (a) Area of 852 × 852 pixels in a 1920 × 1080 SLM is used to record the elemental hologram at uniform beam illumination (the SLM size in the plane of the elemental hologram is MS_{SLM}); (b) SLM active area partitioning into RGB channels for printing the elemental hologram.

irresolvable for a person with a standard visual acuity. The study made in [17] with a holographic stereogram printer and elemental holograms varying in size from 0.05 × 0.05 mm^2 to 0.4 × 0.4 mm^2 proves that the angular resolution provided by the size of 0.05 × 0.05 mm^2 is about 1 degree.

The photographs of optical reconstructions from printed holograms of two objects are shown in Fig. 8 and Fig. 9. We used color computer graphic models of a bunch of flowers and a toy car as 3D contents to build a set of point clouds with large number of points at the recording wavelengths. For example, the number of points in each point cloud built for the first object was about 15 thousands. The holographic fringe patterns for each elemental hologram

in both cases were generated by the FPAS method. They were sequentially recorded onto the holographic emulsion. The size of the printed holograms was 5 cm × 5 cm. The total writing time of the holograms was 9540 s. In the case of conventional mosaic delivery the writing time is 8880 s. It should be noted that at greater laser power one can use more pixels in the SLM or its whole active area to record an elemental hologram with a fragment size of 0.127 mm × 0.127 mm. Thus the writing time will decrease. The recorded color holograms can be displayed by a white light source such as a halogen lamp or a white LED. We see that the printed holograms provide acceptable color quality with bright saturated colors as it should be in the case of mosaic recording. However, no grid artifacts which may be caused by the conventional color partitioning recording method are seen. Figure 9 shows the optical reconstruction of the toy car from different viewpoints, and it is seen that the printed hologram provides both vertical and horizontal parallax (Media 1). As a further improvement of the printing, we plan to study more thoroughly the impact the size of the elemental hologram makes on the quality of reconstruction.

Fig. 8. Photograph of optical reconstruction from a hologram printed by a color wavefront printer with spatial partitioning of the SLM.

5. Conclusion

In summary, we propose a spatial partitioning of the SLM in a full color holographic wavefront 3D printer. The SLM is used to display CGHs which are generated for a 3D object observed from multiple viewpoints. By optical processing of the light waves diffracted by the CGHs on the SLM, the optical wavefronts scattered from the 3D object in multiple directions are extracted and recorded in succession as elemental volume holograms to build a white light viewable reflection hologram. This is done by means of a motorized X-Y stage. The SLM partitioning is applied in order to allow for mosaic delivery of exposures for primary colors when recording a full color hologram. Thus the elemental hologram is formed as a 2D array of R, G, B sub-elemental holograms whose size is scalable according to application and can be made small for smooth color reproduction without high-end optical components. The method is discussed for a 3 × 3 partitioning scheme which results in an elemental hologram built as a mosaic of 9 non-overlapping color patches recorded at the wavelengths of the primary colors. Color recordings are made in succession but increase in the writing time is insubstantial in comparison to the conventional mosaic delivery of exposures when an elemental hologram carries a single color. The method is experimentally verified by printing full-color holograms of 3D objects from point clouds by using a wavefront printer with extraction and demagnification of the first diffraction order. For additional decrease of the elemental hologram size, the latter is formed by using approximately one third of the SLM pixels. A fast phase-added ste-

reogram approach was used for generation of CGHs. The printed color holograms show bright seamless reconstruction and both vertical and horizontal parallax. As a whole, the result looks very encouraging especially in view that wavefront printing is still at its infancy stage. Furthermore, the proposed method makes possible easier color quality improvement than for the color overlap recording method because each RGB color fringe pattern is recorded into different place individually.

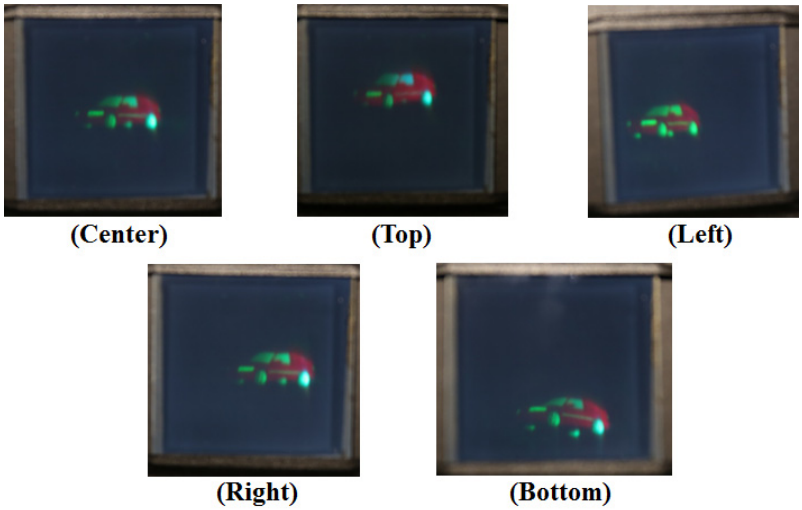

(a)

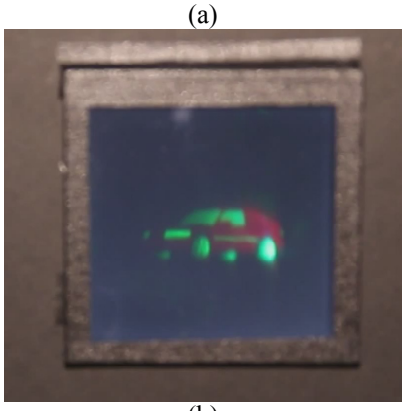

(b)

Fig.9. (a) Photographs of optical reconstructions from a hologram of a toy car printed by a color wavefront printer with spatial partitioning of the SLM; the viewpoints are indicated below the photographs; (b) Movie file recorded by varying the perspective (Media 1)..

Acknowledgment

This work was supported by the IT R&D program “Fundamental technology development for digital holographic contents” of MSIP-Korea.